Inorganic Chemistry

Article

pubs.acs.org/IC

Multimetallic Complexes Featuring a Bridging *N*-heterocyclic Phosphido/Phosphenium Ligand: Synthesis, Structure, and Theoretical Investigation

Baofei Pan, Deirdra A. Evers-McGregor, Mark W. Bezpalko, Bruce M. Foxman, and Christine M. Thomas*

Department of Chemistry, Brandeis University, 415 South Street, Waltham, Massachusetts 02454, United States

Supporting Information

ABSTRACT: By incorporating an N-heterocyclic phosphenium/phosphide (NHP) ligand into a chelating pincer ligand framework (PPP^+/PPP^-), we have elucidated several different and unprecedented binding modes of NHP ligands in homobimetallic, heterobimetallic, and trimetallic metal complexes. One-electron reduction of the previously reported $(PPP)^-/M^{II}$ complexes (PPP)M-Cl (M = Pd (**1**), Pt (**2**)) results in clean formation of the symmetric homobimetallic M^I/M^I complexes $[(\mu\text{-PPP})Pd]_2$ (**5**) and $[(\mu\text{-PPP})Pt]_2$ (**6**). The tridentate NHP ligand has also been utilized as a bridging linker in the M/Co heterobimetallic compounds $(OC)_3Co(u\text{-PPP})M(CO)$ (M = Pd (**7**), Pt (**8**)), synthesized via salt elimination from mixtures of **1** and **2** and $Na[Co(CO)_4]$. Furthermore, an NHP-bridged trimetallic complex $(PPP)_2Pd_3Cl_2$ (**9**) can be synthesized in a manner similar to precursor **1** ($Pd(PPh_3)_4$ + (PPP)Cl) via careful adjustment of reaction stoichiometry. Examination of the interatomic distances and angles in complexes **5**–**9**, in tandem with density functional theory calculations have been used to evaluate and characterize the bonding interactions in these complexes.

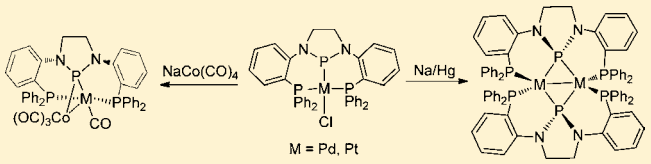

INTRODUCTION

While Arduengo-type *N*-heterocylic carbenes (NHCs)[1,2] have received an extraordinary level of attention in the field of transition metal chemistry[3−5] and organo-catalysis,[6,7] far less focus has been placed on their isovalent group 15 analogues *N*-heterocyclic phosphenium cations (NHP^+s).[8,9] In contrast to NHCs, which are considered to be strong σ-donors and weak π-acceptors in coordination chemistry, theoretical investigation suggests that *N*-heterocyclic phosphenium cations' bonding is dominated by π-acceptor character, with only weak σ-donation to metal centers.[10−12] The electronically inverse properties of these two ligand families suggests reciprocal reactivity in transition metal chemistry. One of the most interesting aspects of NHPs is their ability to potentially adopt different transition metal binding modes in a manner analogous to nitrosyls: NHPs typically adopt a planar binding mode in which the central phosphorus acts as a σ-donor and π-acceptor as a part of phosphenium NHP^+/M^n interaction, but NHPs can also adopt a pyramidal coordination mode in which the two coordinate central phosphorus acts as an anionic X-type ligand as part of a phosphido NHP^-/M^{n+2} interaction.[13] Rosenberg recently reviewed the features and reactivity of both phosphide and phosphenium ligands in the context of the analogy to Schrock vs Fischer carbenes.[14]

Recently, our group developed the first example of a pincer ligand in which an NHP unit is incorporated into the central position of a chelating diphosphine framework.[15] Interestingly, we found that the coordination of this pincer NHP-diphosphine ligand to electron rich metal fragments such as $NaCo^{-I}(CO)_4$ or $M^0(PPh_3)_4$ (M = Pd, Pt) resulted in complexes with an unusual pyramidal geometry about the central NHP unit.[13,16,17] Structural and computational investigations revealed that this geometry was indicative of a stereochemically active lone pair at the phosphorus atom, and thus an NHP^- phosphido description in which the metal centers have been formally oxidized by two electrons. For example, treatment of the phosphorus chloride precursor to the chelating NHP-diphosphine ligand with $M(PPh_3)_4$ results in oxidative addition of the P−Cl bond to form the NHP^--phosphido square planar M^{II}-Cl complexes (PPP)M-Cl (M = Pd (**1**), Pt (**2**), Scheme 1).[13] It was predicted computationally

Scheme 1

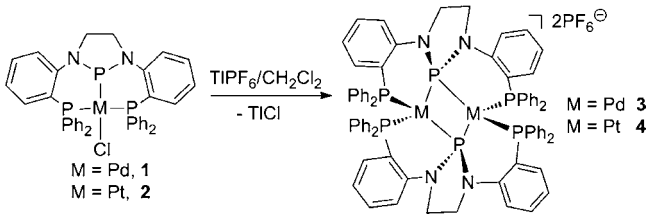

that two-electron oxidation of these M^{II} complexes occurs at the phosphorus center, leading to a planar NHP^+-phosphenium ligand. Incorporation of an NHP donor into a chelating pincer framework has proven advantageous in stabilizing transition metal species with different NHP binding modes, allowing the interconversion between NHP^- phosphido and NHP^+

Received: May 22, 2013
Published: August 7, 2013

   dx.doi.org/10.1021/ic4012873 | *Inorg. Chem.* 2013, 52, 9583−9589

phosphenium configurations,[13] similar to the archetypical non-innocent nitrosyl (NO^+/NO^-) ligand.[18]

In addition to the two terminal binding modes that describe most NHP complexes, our pincer-type NHP ligand can also bridge two metals (Scheme 1).[13] Halide abstraction from M^{II} complexes **1** and **2** results in isolation of asymmetric dimers $[(PPP)M]_2[PF_6]_2$ (M = Pd (**3**), Pt (**4**)). The NHP unit in these complexes is best described as an NHP^+ phosphenium ligand accepting electron density from one metal center and donating a lone pair to the second metal center, similar to a semibridging carbonyl ligand. In line with this, the Pd and Pt centers in **3** and **4** adopt tetrahedral geometries, indicative of reduced Pd^0 and Pt^0 oxidation states, respectively. Compound **3** and **4** joined just one other reported example of a complex featuring asymmetrically bridging NHP^+ cations: $Co_2(CO)_5(\mu\text{-}NHP^{Me})_2$.[19] A very recent report by Gudat and co-workers has also shown that monodentate NHP^+ ligands asymmetrically bridge in the Pd and Pt complexes $[(NHP)MCl]_2$ (M = Pd, Pt).[20] Furthermore, an unsymmetrical bridging mode was described for $[(NHP)NiCl]_2$ by Baker and co-workers, and the NHP^+ phosphenium description was supported by electrochemical studies.[21]

NHP^- phosphido ligands are also expected to adopt bridging modes in bimetallic complexes owing to their accessible stereochemically active lone pair allowing a *symmetric* bridging mode, similar to more traditional R_2P^- phosphidos. However, there is only one example of a symmetrically bridging N-heterocyclic phosphide ligand in the literature, an Os–Rh cluster in which the NHP unit symmetrically bridges two Os centers.[22] There are, on the other hand, several examples of metal complexes containing acyclic $\mu\text{-}P(NR_2)_2^-$ ligands that bridge in an asymmetric, μ-phosphido fashion.[23−28] Since our NHP-containing diphosphine pincer ligand has already proven to asymmetrically bridge Pd and Pt centers in homobimetallic compounds **3** and **4**, we now turn our attention to other possible binding modes as a phosphido bridging ligand in both homo- and heterobimetallic as well as trimetallic complexes.

RESULTS AND DISCUSSION

NHP-Bridged M/M Homobimetallic Complexes (M = Pd, Pt). We first examined the ability to interconvert NHP^+/NHP^- binding modes via redox chemistry. One-electron reduction of (PPP)Pd–Cl (**1**) with 1.1 equiv of 1% Na/Hg amalgam in tetrahydrofuran (THF) at room temperature for 12 h generates the Pd^I/Pd^I dimer complex **5** $[(\mu\text{-PPP})Pd]_2$, as shown in Scheme 2. The ^{31}P NMR spectrum of complex **5** features a downfield signal at 297.2 ppm and an upfield shift at 23.3 ppm in a 1:2 integral ratio, which is in agreement with a Pd-bound NHP unit and two symmetrically coordinated aryl phosphine arms.

Scheme 2

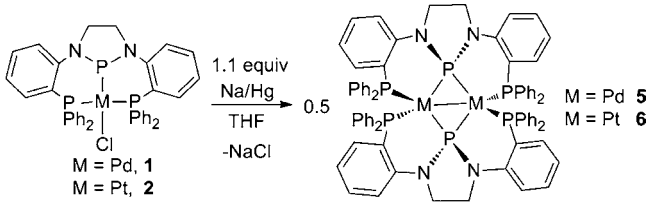

As shown in Figure 1, the solid state structure of **5** confirms the formulation as a homobimetallic Pd complex with two symmetrically bridging NHP-diphosphine ligands. The distances between the central NHP phosphorus atoms and each Pd center are quite similar (Pd1–P2, 2.3026(9) Å; Pd1–P5, 2.2933(8) Å; Pd2–P2, 2.2816(8) Å; Pd2–P5, 2.3023(8) Å), and are substantially longer than the $P^{(NHP)}$-Pd multiple bond distance in the NHP^+ phosphenium bridged dimer complex **3** $[(PPP)Pd]_2[PF_6]_2$ (2.1242(16) Å).[13] The $P^{(NHP)}$-Pd distances in **5** are, however, comparable with the P–Pd distances in reported bis(phosphide)-bridged Pd(I) dimers (2.23–2.33 Å),[29−34] suggesting that the bridging NHP ligand in complex **5** is best described as an NHP^- phosphido bridging ligand. The tetrahedral geometry of the central NHP phosphorus atoms and Pd centers, as well as the bent angle between the N–P–N plane and each P–Pd bond vector (average 145.6°) are consistent with the assignment as a $\mu\text{-}NHP^-$ phosphido Pd(I) dimer complex. Diamagnetic complex **5** is best assigned as a Pd(I)Pd(I) dimer with a direct metal–metal σ interaction, resulting in a Pd–Pd distance of 2.6972(3) Å. While this distance is shorter than the sum of the covalent radii of two Pd centers (2.75 Å),[35] other bis(phosphide)-bridged Pd(I) dimers in the literature have significantly shorter Pd–Pd contacts (2.57–2.62).[29−34] The key differences between **5** and the known literature compounds are the increased coordination number at Pd (two ancillary phosphine ligands bound to each Pd in **5**, compared to just one monodentate phosphine in other phosphide-bridged Pd(I)Pd(I) dimers), as well as the chelating nature of the phosphide ligand and the resulting constraints imposed by the ligand.

In a similar reaction, reduction of the platinum derivative (PPP)Pt–Cl (**2**) with Na/Hg amalgam results in the formation of a neutral Pt(I) dimer complex $[(\mu\text{-PPP})Pt]_2$ (**6**, Scheme 2). Complex **6** features a downfield shift at 241.9 ppm and an upfield signal at 10.3 ppm with $^1J_{Pt-P}$ coupling constants 2250 and 4790 Hz, respectively, suggesting the coordination of both NHP and aryl phosphine arms to the Pt centers. These chemical shifts and coupling constants are similar to those observed for the dicationic dimer complex $[(\mu\text{-PPP})Pt]_2$ (**4**) (δ_{NHP} 257.5 ppm, $^1J_{Pt-P}$ = 2160 Hz),[13] implying similar strength of the Pt–P interaction.

As shown in Figure 1, the structure obtained via X-ray diffraction of single crystals of **6** is very symmetric with four identical $P^{(NHP)}$-Pt bond distances (2.2827(4) Å). Again, the Pt–P distances associated with the bridging NHP unit are longer than the $P^{(NHP)}$-Pt multiple bond distance (2.126(2) Å) in the NHP^+ phosphenium bridged dimer complex **4** $[(PPP)Pt]_2[PF_6]_2$.[13] All of the structural features (i.e., the geometries about the NHP phosphorus and Pt centers) suggest that the conclusions drawn about **5** also apply to complex **6**, and that this compound is also best described as an NHP^- phosphide-bridged Pt(I) dimer with a direct Pt–Pt σ bond interaction. The Pt–Pt distance in **6** is 2.7640(16) Å, which is essentially equal to the sum of the covalent radii of two Pt atoms (2.77 Å).[35] This intermetallic distance is longer than that observed for other structurally characterized bis(phosphido)-bridged Pt(I)Pt(I) complexes in the literature (2.59–2.64 Å).[34,36−40] As postulated for complex **5** (vide supra), this long intermetallic distance may be the result of steric constraints imparted by the ligand.

NHP-Bridged M/Co Heterobimetallic Complexes (M = Pd, Pt). In addition to acting as bridging ligands in homobimetallic complexes, we were curious to ascertain if the versatility of our NHPs would allow them to bridge two different metal centers in heterobimetallic complexes. As shown

dx.doi.org/10.1021/ic4012873 | Inorg. Chem. 2013, 52, 9583–9589

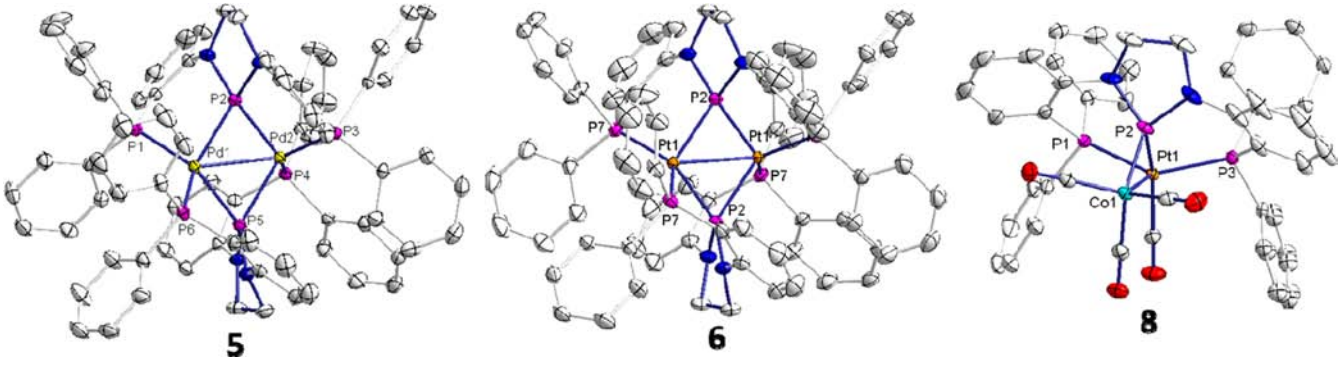

Figure 1. Displacement ellipsoid (50%) representations of **5**, **6**, and **8**. For clarity, all hydrogen atoms and solvate molecules are omitted. Relevant interatomic distances (Å) and angles (deg): **5**: Pd1−Pd2, 2.6972(3); Pd1−P2, 2.3026(9); Pd1−P5, 2.2933(8); Pd2−P2, 2.2816(8); Pd2−P5, 2.3023(8). **6**: Pt1−Pt1, 2.7640(16); Pt1−P2, 2.2827(4). **8**: Pt1−P2, 2.2252(5); Co1−P2, 2.1026(5); Pt1−Co1, 2.8008(3); Pt1−P2−Co1, 80.603(15).

in Scheme 3, treatment of **1** or **2** with $NaCo(CO)_4$ at room temperature affords M/Co heterobimetallic complexes

Scheme 3

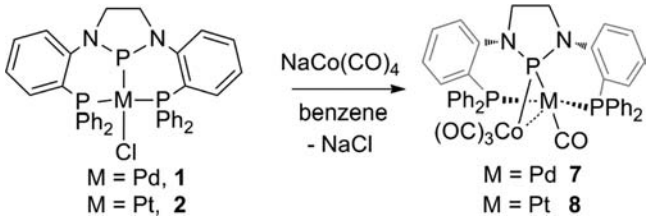

$(OC)_3Co$(u-PPP)M(CO) (M = Pd (**7**), Pt (**8**)), in which the NHP ligand bridges the two metals. The ^{31}P NMR spectrum of each complex features a downfield signal (289.7 ppm, **7**; 269.0 ppm, **8**) and an upfield shift (1.5 ppm, **7**; −9.3 ppm, **8**) in a 1:2 integral ratio, corresponding to the coordinated NHP unit and phosphine arms, respectively. The equivalent ^{31}P NMR shifts of the pendant triaryl phosphines and the large side arm P^{Ar}-Pt coupling constant ($^1J_{Pt-P}$ = 3705 Hz) in **8** suggest that both phosphine arms remain coordinated to the Pt center. The P^{NHP}-Pt coupling constant remains quite large ($^1J_{Pt-P}$ = 1890 Hz) and similar to the value observed for the symmetric homobimetallic dimer **6**.

The formulation of these complexes was further confirmed by an X-ray diffraction study on single crystals of **8** (Figure 1, complex **7** is assumed to be structurally similar to **8**). In contrast to the homobimetallic complexes **3**−**6** in which the two phosphine side arms from the same pincer framework span two different metal centers, the two phosphine arms in **8** remain coordinated only to the Pt center, while the NHP unit bridges the Pt and Co atoms. Similar to the NHP units in complexes **5** and **6**, the central NHP phosphorus atom in **8** adopts a tetrahedral geometry with asymmetric bent angles between the N−P−N plane and each $P^{(NHP)}$-M (M = Pt, Co) bond vector (131.2° between N−P−N plane and Pt−P bond vector; 148.2° between N−P−N plane and Co−P bond vector). The Pt−$P^{(NHP)}$ distance in **8** (2.2252(5) Å) is shorter than that in phosphide-bridged complex **6** (2.2827(4) Å) and longer than the shorter of the two distances in the asymmetric Pt dimer **4** (2.126(2) Å),[13] but compares well with the Pt−P distances in $[(PPP)Pt(PPh_3)]PF_6$ (2.2600(7) Å), $[(PPP)Pt(PMe_3)]PF_6$ (2.2606(9) Å), and (PPP)PtBr (2.2446(11) Å).[13] This would imply NHP^- Pt(II) phosphido character, but other structural data is inconsistent with this assignment. For instance, the geometry about the Pt center is distorted tetrahedral, inconsistent with a Pt^{II} assignment. Moreover, the $P^{(NHP)}$-Co distance (2.1026(5) Å) is quite short compared to the $P^{(NHP)}$-Co single bond distance (2.2386(6) Å) in the pyramidal NHP^- phosphido-cobalt complex $(PPP)Co(CO)_2$.[16] Indeed, the particularly short $P^{(NHP)}$-Co distance in **8** is more similar to the $P^{(NHP)}$-Co multiple bond distance in an asymmetric NHP-bridged $Co_2(CO)_5(\mu\text{-}NHP^{Me})_2$ dimer reported by Paine and co-workers (2.051(1) Å and 2.043(1) Å),[19] suggesting strong Co−$P^{(NHP)}$ bonding in **8**. There are no structurally characterized phosphorus donor-bridged Co/Pt or Co/Pd bimetallic compounds in the literature for comparison. It is also pertinent to comment on the relatively long Co−Pt interatomic distance of 2.8008(3) Å in **8** (sum of covalent radii of Co and Pt = 2.64 Å).[35] The Co−Pt distances in structurally characterized Co/Pt complexes range from (2.40 to 2.75).[41−56] The comparatively long Co−Pt distance in **8** indicates the absence of a covalent metal−metal interaction, although a weak donor/acceptor interaction is possible.

Another interesting feature of **7** and **8** is that one of the CO ligands from the $Co(CO)_4^-$ fragment has migrated to the Group 10 metal center. Three ν(CO) stretches are observed in the IR spectrum of each complex (**7**: 2046, 1988, 1924 cm^{-1}; **8**: 2020, 1985, 1920 cm^{-1}). While these stretches are inherently vibrationally coupled, making comparisons difficult, the latter two stretches are very similar to those in a pincer (NHP-diphenylphosphino)-Co^I monomer compound reported by our group (1981 and 1926 cm^{-1}).[16] For comparison, a series of Pt^{II}/Co^{-1} carbonyl complexes $(PPh_3)(R)(CO)Pt-Co(CO)_3(PPh_3)$ were reported to have ν(CO) stretches over a much wider range (2049−1887 cm^{-1}), perhaps indicating different metal oxidation states than **7** and **8**.[41]

Given the short Co−$P^{(NHP)}$ distance and the tetrahedral geometry at the Pt center, there are two bonding descriptions available to accurately describe complexes **7** and **8**: (1) The NHP acts as an X-type NHP^- phosphido ligand to Co^I and an L-type ligand via lone pair donation to Pt^0. (2) The NHP acts as an NHP^+ phosphenium ligand toward Co^{-I} and interacts with Pt^0 via accepting electron density into the vacant p orbital on phosphorus. The latter bonding situation might give rise to a weak Co→Pt donor−acceptor interaction, while the former might be more likely to lead to a Pt→Co donor−acceptor interaction.

dx.doi.org/10.1021/ic4012873 | Inorg. Chem. 2013, 52, 9583−9589

To further investigate these possibilities, complex **8** was studied computationally using density functional theory (DFT) and natural bond orbital (NBO) methods. Geometry optimization of **8** led to a core geometry quite similar to that derived from X-ray crystallography (see Supporting Information). Subsequent NBO analysis revealed a Pt−$P^{(NHP)}$ NBO with 73.3% contribution from the phosphorus atom and 26.7% contribution from Pt, indicative of a dative P→Pt bond. In contrast, the Co−$P^{(NHP)}$ NBO was found to be essentially covalent, with nearly equal contributions from both Co and P (44.1% and 55.9%, respectively). These NBOs are depicted in Figure 2. In addition to these bonds, NBO analysis reveals a

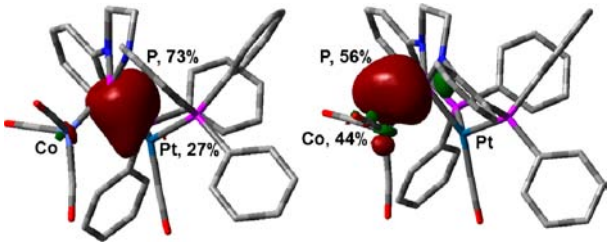

Figure 2. Visual representation of the calculated $P^{(NHP)}$-Pt (left) and $P^{(NHP)}$-Co (right) NBO surfaces (B3LYP/LANL2DZ).

strong (E^{del} = 156.9 kcal/mol) donor−acceptor interaction between the $P^{(NHP)}$-Pt bonding orbital and an empty orbital on Co (Figure 3, left). This interaction accounts for the strong

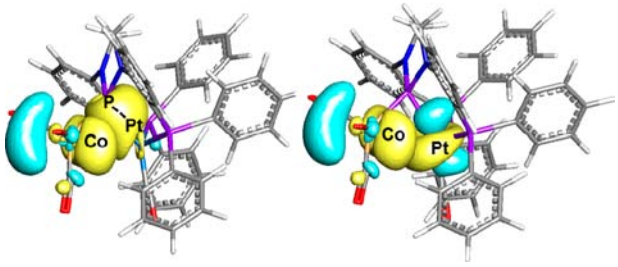

Figure 3. Pictorial representations of the calculated donor−acceptor interactions (NBO analysis) between the $P^{(NHP)}$-Pt bonding orbital and an empty orbital on Co (left) and from a filled orbital on Pt to an empty orbital on Co (right).

multiple bonding between the central NHP phosphorus atom and the Co center suggested by the short Co−P distance in **8**. In addition, NBO methods revealed a weaker (E^{del} = 18.0 kcal/mol) Pt→Co donor−acceptor interaction (Figure 3, right). Thus, computational results support the first of the aforementioned possible bonding descriptions of **8**, namely, as a Pt^0/Co^I heterobimetallic complex with a bridging NHP^--phosphido ligand with a weak Pt→Co interaction.

NHP-Bridged Trimetallic Pd Complex. NHP-containing pincer ligands have also been shown to bridge three metal centers in a Pd trimetallic complex. In a procedure similar to the synthesis of complex **1**,[13] treatment of the chlorophosphine ligand precursor (PPP)Cl with 1.5 equiv of $Pd(PPh_3)_4$ affords the asymmetric trimetallic complex $(PPP)_2Pd_3Cl_2$ (**9**, Scheme 4). The structure of complex **9** was elucidated using single crystal X-ray diffraction (Figure 4). Despite the apparent inequivalence of all three phosphorus atoms of each ligand in the solid state, the ^{31}P NMR spectrum of complex **9** reveals only two resonances at 299.3 and 10.9 ppm in a 1:2 integral

Scheme 4

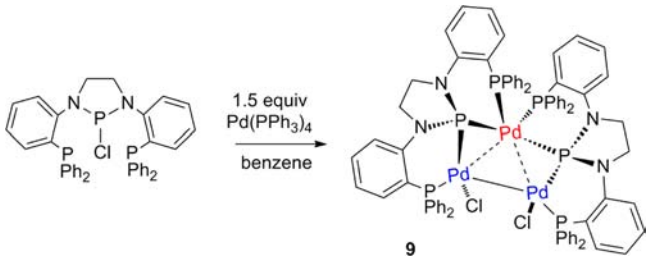

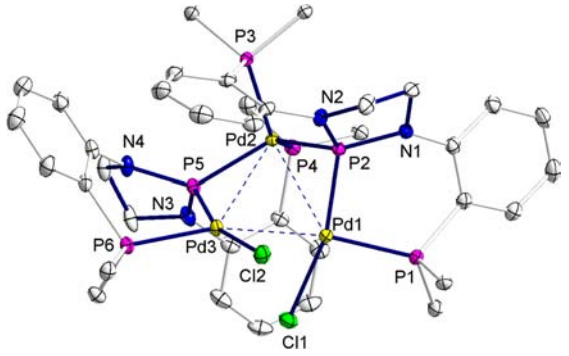

Figure 4. Displacement ellipsoid (50%) representation of **9**. For clarity, all hydrogen atoms, solvate molecules, and phenyl groups on the phosphine side arms are omitted. Relevant interatomic distances (Å): Pd1−Pd2, 2.8918(3); Pd1−Pd3, 2.7007(3); Pd2−Pd3, 2.9464(3); Pd1−P1, 2.2599(6); Pd1−P2, 2.1675(6); Pd2−P2, 2.2887(6); Pd2−P3, 2.3095(6); Pd2−P4, 2.3786(6); Pd2−P5, 2.2556(5); Pd3−P5, 2.1806(6); Pd3−P6, 2.2530(6).

ratio. The phosphine side arms should be in chemically different environments, suggesting that the single broad resonance observed at 10.9 ppm is either the result of accidental overlap of two independent resonances or a fluxional process occurring in solution at room temperature. Notably, variable temperature (rt to −60 °C) ^{31}P and ^1H NMR spectroscopy does reveal splitting and sharpening of resonances as the temperature is lowered, characteristic of decoalescence behavior. However, at this point, the nature of the fluxional process occurring in solution is unknown.

The solid state structure of complex **9**, which reveals that the two Pd−Cl bond vectors are aligned antiparallel to each other, provides some insight into the electronic description of this complex (Figure 4). The NHP-phosphorus atoms each have shorter Pd−P distances associated with the chloride-bound Pd centers (2.1806(6) Å and 2.1675(6) Å), while the bonds to the third Pd center are substantially longer (2.2887(6) Å and 2.2556(5) Å). The angles between the N−P−N planes and the Pd−P bond vectors are also not equal (e.g., angles between N1−P2−N2 plane and Pd2 and Pd1 = 148° and 136°, respectively). Moreover, it is interesting to note that the distances between the pendent phosphines and the Pd centers differ significantly, with the chloride-bound Pd ions binding more tightly to the phosphines (2.2530(6) Å and 2.2599(6) Å) than the third Pd center (2.3095(6) Å and 2.3786(6) Å). All of this structural information allows two conclusions to be drawn: (1) of the three Pd centers, Pd2 appears to be electronically different from Pd1 and Pd3, and (2) the NHP units bind in a different fashion to Pd2 than they do to Pd1 and Pd3. It is also important to note that while two of the Pd−Pd contacts appear too long for significant metal−metal interactions, the distance

dx.doi.org/10.1021/ic4012873 | Inorg. Chem. 2013, 52, 9583−9589

between the Cl-bound Pd centers, Pd1 and Pd3, is 2.7007(3) Å and in the same range as that seen in complex **5**. Several phosphido-bridged trimetallic Pd complexes have been structurally characterized, including $[Pd_3^{4+}]$[31,57−59] and $[Pd_3^{6+}]$[60,61] examples. Of these, the triangular mixed-valence $[Pd_3(\mu_2\text{-}PR_2)_2(\mu_2\text{-}Cl)(PR'_3)_3]^+$ complexes are the most similar to **9**, and also feature somewhat asymmetrically bridging phosphido ligands; however, the Pd−P distances associated with the bridging PR_2^- ligands in these complexes are significantly longer (2.2−2.28 Å).[58] It is tempting to simply consider complex **9** as the result of insertion of a Pd^0 center into two molecules of Pd^{II} monomer **1**, particularly since addition of 1 equiv of (PPP)Cl to **9** leads to quantitative conversion to **1** (presumably via oxidative addition of the P−Cl bond to the purported Pd^0 center). Nonetheless, further investigation into this hypothesis was deemed necessary.

To better understand the bonding in complex **9**, we again turned to computational, specifically NBO, methods. The geometry of **9** was optimized starting from crystallographically determined coordinates, leading to a structure with bond metrics similar to those determined in the solid state (see Supporting Information). Subsequent NBO analysis revealed significant differences between the bonding of the μ-NHP and the two different types of Pd centers in complex **9**. The bonding between the NHP unit and the chloride-bound Pd centers was shown to be covalent, with a ∼50% contribution from each atom to the Pd−P NBO (Figure 5, left). In contrast,

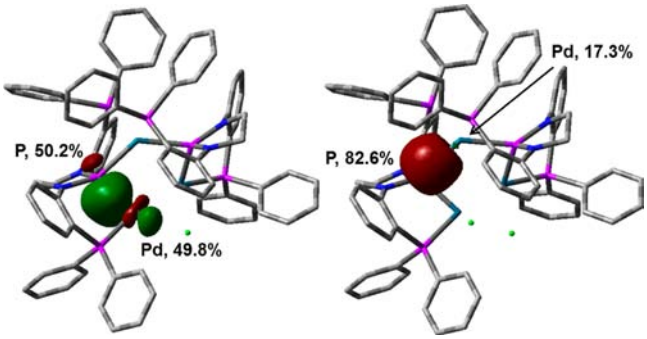

Figure 5. Visual representation of the calculated $P^{(NHP)}$-Pd-Cl (left) and $P^{(NHP)}$-$Pd_{central}$ (right) NBO surfaces (B3LYP/LANL2DZ) with labeled with % contributions from each atom.

the NHP engages in dative P→Pd bonding with the third inequivalent Pd center, with much more phosphorus character to this Pd−P NBO (82.6% P, 17.3% Pd; Figure 5, right). These results lead to the conclusion that the bridging NHP in complex **9** is best described as a bridging NHP^- phosphido ligand covalently bound to two Pd^{II}−Cl centers and datively donating to one Pd^0 center. In line with this assignment, the two halide-bound Pd centers adopt a distorted square planar geometry (Pd1 and Pd3) while the third Pd center is distorted tetrahedral (Pd2). Further, the natural charges computed by NBO suggest that the halide-bound Pd centers are more positively charged (−0.1) than the third Pd center (−0.67), consistent with a $Pd^{II}/Pd^{II}/Pd^0$ description.

CONCLUSION

In summary, we have presented several new bridging modes of *N*-heterocyclic phosphido ligands in homo- and heterobimetallic complexes as well as trimetallic clusters. Depending on the nature of the metal centers bridged by the NHP, these ligands can adopt either a symmetrically or asymmetrically bridging geometry. First, the reduction of the Group 10 NHP^- phosphido complexes $(PPP)M^{II}$-Cl allows the generation of pincer NHP-diphosphine M^I (M = Pd, Pt) dimer complexes symmetrically bridged by two NHP^- units. These M^I/M^I complexes appear to have direct metal−metal interactions. In addition to these homobimetallic complexes, extrusion of NaCl via the reaction between (PPP)M-Cl (M = Pd, Pt) and $NaCo(CO)_4$ results in the formation of heterobimetallic complexes featuring unsymmetrically bridging NHP units. Both the experimental observations and the theoretical calculations suggest NHP^- phosphido character for the NHP moiety in the new heterobimetallic Pt/Co and Pd/Co compounds. However, in this case, a formal two-electron redox reaction appears to have occurred between the metal centers, generating products that are best described by the M^0/Co^I combination of oxidation states. Lastly, the NHP-diphosphine ligand has also been used to construct a trimetallic NHP-bridged complex $(PPP)_2Pd_3Cl_2$ (**9**). Structural and theoretical investigations also suggest an NHP^- phosphido description for the bridging NHP units in this complex, which can best be thought of as forming via insertion of a bridging Pd^0 center into two molecules of the Cl−Pd^{II} NHP^- phosphido complex **1**.

Further investigations will focus on the reactivity of these unusual molecules, as well as expansion of the coordination chemistry of the NHP-diphosphine ligand to other transition metals in mono- and multimetallic complexes.

EXPERIMENTAL SECTION

General Considerations. All syntheses reported were carried out using standard glovebox and Schlenk techniques in the absence of water and dioxygen, unless otherwise noted. Benzene, *n*-pentane, tetrahydrofuran, toluene, diethyl ether, and dichloromethane were degassed and dried by sparging with ultra high purity argon gas followed by passage through a series of drying columns using a Seca Solvent System by Glass Contour. All solvents were stored over 3-Å molecular sieves. Deuterated benzene and dichloromethane were purchased from Cambridge Isotope Laboratories, Inc., degassed via repeated freeze−pump−thaw cycles, and dried over 3-Å molecular sieves. Solvents were frequently tested using a standard solution of sodium benzophenone ketyl in tetrahydrofuran to confirm the absence of oxygen and moisture. Complexes (PPP)Cl,[15] (PPP)Pd−Cl (**1**),[13] (PPP)Pt−Cl (**2**),[13] $[(PPP)Pd]_2[PF_6]_2$ (**3**),[13] $[(PPP)Pt]_2[PF_6]_2$ (**4**),[13] and $NaCo(CO)_4$[62] were synthesized following literature procedures. All other chemicals were purchased from Aldrich, Strem, or Alfa Aesar and used without further purification. NMR spectra were recorded at ambient temperature unless otherwise stated on a Varian Inova 400 MHz instrument. ^1H and ^{13}C NMR chemical shifts were referenced to residual solvent and are reported in ppm. ^{31}P NMR chemical shifts (in ppm) were referenced to 85% H_3PO_4 (0 ppm). Elemental microanalyses were performed by Complete Analysis Laboratories, Inc., Parsippany, NJ.

[(μ-PPP)Pd]$_2$ (5). To a suspension of 1% Na/Hg amalgam (3.06 mg Na, 0.133 mmol) in THF (5 mL) was added a yellow solution of **1** (91.0 mg, 0.121 mmol) in THF (2 mL). The mixture was allowed to stir for 12 h to ensure complete reaction, then the dark green solution was collected via filtration through Celite. Removal of the volatiles in vacuo afforded dark green solid residue as the crude product. The crude product was redissolved in minimal THF and slow diffusion of *n*-pentane into this solution afforded dark green crystals suitable for single crystal X-ray diffraction. Yield: 49.0 mg, 56.5%. ^1H NMR (400 MHz, CD_2Cl_2): δ 7.20 (m, 4H, Ar-*H*), 7.15−7.11 (m, 10H, Ar-*H*), 6.87 (br, 4H, Ar-*H*), 6.78 (t, 6H, Ar-*H*), 6.43 (br, 2H, Ar-*H*), 6.93 (m, 2H, Ar-*H*), 3.40 (m, 4H, CH_2). ^{31}P NMR (161.8 MHz, CD_2Cl_2): δ 297.2 (br, 1P), 23.3 (br, 2P). Because of the poor solubility of **5**, ^{13}C

dx.doi.org/10.1021/ic4012873 | Inorg. Chem. 2013, 52, 9583−9589

NMR was not collected. Anal. Calcd for $C_{76}H_{64}N_4P_6Pd_2$: C, 63.74; H, 4.50; N, 3.91. Found: C, 63.25; H, 4.49; N, 3.81.

[(μ-PPP)Pt]$_2$ (6). A similar procedure to that described for **5** was followed, using **2** (52.6 mg, 0.0626 mmol) and 1% Na/Hg amalgam (1.6 mg Na, 0.0689). Single crystals suitable for X-ray diffraction were obtained via the diffusion of diethyl ether into a concentrated THF solution of crude red/orange **6**. Yield: 32.1 mg, 63.8%. ^{1}H NMR (400 MHz, C_6D_6): δ 7.39 (m, 4H, Ar-*H*), 7.18 (br, 4H, Ar-*H*), 7.04 (t, 4H, Ar-*H*), 6.99 (m, 4H, Ar-*H*), 6.91 (t, 2H, Ar-*H*), 6.83 (m, 2H, Ar-*H*), 6.71 (t, 4H, Ar-*H*), 6.51 (t, 2H, Ar-*H*), 6.41 (m, 2H, Ar-*H*), 3.19 (m, 2H, C*H*$_2$), 2.80 (m, 2H, C*H*$_2$). ^{31}P NMR (161.8 MHz, C_6D_6): δ 241.9 (br, 1P, $^1J_{Pt-P}$ = 2250.0 Hz, $^2J_{P-P}$ = 26.7), 10.3 (dt, 2P, $^1J_{Pt-P}$ = 4753.9 Hz, $^2J_{P-P}$ = 26.7 Hz). Because of the poor solubility of **6**, ^{13}C NMR was not collected. Anal. Calcd for $C_{76}H_{64}N_4P_6Pt_2$: C, 56.72; H, 4.01; N, 3.78. Found: C, 56.77; H, 4.07; N, 3.42.

(OC)$_3$Co(μ-PPP)Pd(CO) (7). To a white suspension of $NaCo(CO)_4$ (16.4 mg, 0.0832 mmol) in benzene (3 mL) was added a yellow solution **1** (62.5 mg, 0.0832 mmol) in benzene (5 mL). The mixture became red in 30 min. The reaction was allowed to stir overnight at room temperature to ensure completion, and the clear red solution was collected via filtration through Celite. Removal of the volatiles from the filtrate in vacuo afforded a dark red solid as crude product. Crude **7** was dissolved in minimal THF and slow vapor diffusion of *n*-pentane into this solution afforded analytically pure **7** as red crystals. Yield: 72.4 mg, 89.2%. IR (C_6H_6, KBr solution cell): 2046, 1988, 1924 cm^{-1}. ^{1}H NMR (400 MHz, C_6D_6): δ 7.29 (m, 4H, Ar-*H*), 7.16 (m, 2H, Ar-*H*), 7.03−6.99 (m, 6H, Ar-*H*), 6.90−6.87 (m, 8H, Ar-*H*), 6.77 (t, 4H, Ar-*H*), 6.69 (m, 4H, Ar-*H*), 3.32 (m, 2H, C*H*$_2$), 2.14 (m, 2H, C*H*$_2$). ^{31}P NMR (161.8 MHz, C_6D_6): δ 289.7 (t, 1P, $^2J_{P-P}$ = 33.5 Hz), 1.5 (d, 2P, $^2J_{P-P}$ = 33.5 Hz). ^{13}C NMR (100.5 MHz, C_6D_6): δ 212.1 (s, Co(*C*O)$_3$), 195.4 (s, Pd(*C*O)), 147.6 (br s, N-bound *ipso*-Ar), 137.6 (s, P-bound *ipso*-Ar), 137.4 (s, P-bound *ipso*-Ar), 134.9 (d, Ar, J_{P-C} = 15.2 Hz), 133.9 (d, Ar, J_{P-C} = 13.8 Hz) 133.1 (br s, Ar), 131.7 (br s, Ar), 129.4 (br s, Ar), 128.7 (br s, Ar) 125.3 (br s, Ar), 50.1 (s, backbone *C*H$_2$). Anal. Calcd for $C_{42}H_{32}Co_1N_2O_4P_3Pt_1$: C, 56.87; H, 3.64; N, 3.16. Found: C, 56.81; H, 3.55; N, 3.21.

(OC)$_3$Co(μ-PPP)Pt(CO) (8). A procedure identical to that described for complex **7** was followed, using **2** (65.0 mg, 0.0774 mmol) and $NaCo(CO)_4$ (15.0 mg, 0.0774 mmol). Single crystals suitable for X-ray diffraction were obtained via diffusion of *n*-pentane into a concentrated THF solution of red-orange **8**. Yield 62.3 mg, 82.5%. IR (C_6H_6, KBr solution cell): 2020, 1985, 1920 cm^{-1}. ^{1}H NMR (400 MHz, C_6D_6): δ 7.50 (m, 4H, Ar-*H*), 7.24 (m, 4H, Ar-*H*), 7.06 (t, 2H, Ar-*H*), 6.98−6.92 (m, 8H, Ar-*H*), 6.87 (m, 4H, Ar-*H*), 6.80 (t, 4H, Ar-*H*), 6.59 (t, 2H, Ar-*H*), 3.35 (m, 2H, C*H*$_2$), 2.505 (m, 2H, C*H*$_2$). ^{31}P NMR (161.8 MHz, C_6D_6): δ 269.0 (dt, 1P, $^1J_{Pt-P}$ = 1885.2 Hz, $^2J_{P-P}$ = 26.1 Hz), −9.30 (dd, 2P, $^1J_{Pt-P}$ = 3704.9, $^2J_{P-P}$ = 26.1 Hz). ^{13}C NMR (100.5 MHz, C_6D_6): δ 211.7 (s, Co(*C*O)$_3$), 185.8 (d, Pt(*C*O), J_{P-C} = 49.6 Hz, Pt satellites not observed), 147.5 (m, N-bound *ipso*-Ar), 137.8 (t, P-bound *ipso*-Ar, J_{P-C} = 23.7 Hz), 136.9 (t, P-bound *ipso*-Ar, J_{P-C} = 17.5 Hz), 134.1 (t, Ar, J_{P-C} = 7.6 Hz), 133.3 (s, Ar), 132.7 (t, Ar, J_{P-C} = 6.8 Hz), 131.8 (s, Ar), 129.9 (d, Ar, J_{P-C} = 29.7 Hz), 128.8−128.4 (m, Ar), 123.9 (d, Ar, J_{P-C} = 25.1 Hz), 48.7 (s, backbone *C*H$_2$). Anal. Calcd for $C_{42}H_{32}Co_1N_2O_4P_3Pt_1$: C, 51.70; H, 3.31; N, 2.87. Found: C, 51.81; H, 3.25; N, 2.80.

Pd$_3$(μ-PPP)Cl$_2$ (9). Solid $Pd(PPh_3)_4$ (36.0 mg, 0.0312 mmol) was added to a stirring, clear solution of (PPP)Cl (13.4 mg, 0.0208 mmol) in ∼2 mL of benzene. After about 1 min the reaction mixture became dark red. The reaction mixture was stirred at room temperature for 5 min before filtering. The volume of the mother liquor was reduced under vacuum and left at room temperature for crystallization. Analytically pure dark red crystals of **9** formed. Yield: 15.5 mg, 46.4% yield. ^{1}H NMR (400 MHz, C_6D_6): δ 8.38 (br s, 1H, Ar), 7.90 (br m, 1H, Ar), 7.59 (br s, 2H, Ar), 7.50 (d, 2H, Ar, J_{P-C} = 8.0 Hz), 7.40 (m, 14H, Ar), 7.09 (m, 4H, Ar), 7.03 (m, 18H, Ar), 6.86 (t, 4H, Ar, J_{P-C} = 14.4 Hz), 6.76 (t, 2H, Ar, J_{P-C} = 14.4 Hz), 6.68 (br s, 2H, Ar), 6.62 (d, 2H, Ar, J_{P-C} = 6.8 Hz), 6.46 (t, 2H, Ar, J_{P-C} = 15.2 Hz), 6.33 (br s, 2H, Ar), 2.83 (br s, 2H, C*H*$_2$), 2.52 (br s, 2H, C*H*$_2$), 2.21 (br s, 2H, C*H*$_2$), 2.03 (br s, 2H, C*H*$_2$). ^{31}P NMR (161.8 MHz, C_6D_6): δ 299.3 (s, 2P), 10.9 (s, 4P). ^{13}C NMR (100.5 MHz, CD_2Cl_2): δ 149.7 (s, N-bound ipso, Ar), 147.5 (s, N-bound ipso, Ar), 140.3 (br s, P-bound ipso, Ar), 138.1 (br s, P-bound ipso, Ar), 136.1 (s, Ar), 135.4 (s, Ar), 134.0 (d, Ar, J_{P-C} = 19.8 Hz), 133.1 (br s, Ar), 132.2 (br s, Ar), 131.7 (s, Ar), 130.9 (s, Ar), 130.6 (d, Ar, J_{P-C} = 32.1 Hz), 129.3 (s, Ar), 128.7 (br s, Ar), 128.1 (s, Ar), 127.7 (s, Ar), 125.1 (s, Ar), 123,4 (d, Ar, J_{P-C} = 33.6 Hz). Anal, Calcd for $C_{76}H_{64}N_4P_6Cl_2Pd_3$: C, 56.71; H, 4.01; N, 3.4%. Found: C, 56.70; H, 3.89; N, 3.46.

X-ray Crystallography. All operations were performed on a Bruker-Nonius Kappa Apex2 diffractometer, using graphite-monochromated MoKα radiation. All diffractometer manipulations, including data collection, integration, scaling, and absorption corrections were carried out using the Bruker Apex2 software.[63] Preliminary cell constants were obtained from three sets of 12 frames. Crystallographic data and refinement parameters are summarized in Supporting Information, Table S1.

Computational Details. All calculations were performed using Gaussian09[64] for the Linux operating system. DFT calculations were carried out using the B3LYP hybrid functional, Becke's three parameter exchange functional (B3),[65] and the correlation functional of Lee, Yang, and Parr (LYP).[66] A mixed-basis set was employed, using the LANL2DZ(p,d) double-ζ basis set with effective core potentials for phosphorus, cobalt, palladium, platinum, and chlorine[67−69] and Gaussian09's internal LANL2DZ basis set (equivalent to D95 V[70]) for carbon, nitrogen, oxygen, and hydrogen. Basis sets and functionals were chosen based on methods that had previously proven successful with other NHP complexes and were optimized for computational time and accuracy.[13,16,17] Using crystallographically determined geometries as a starting point, the geometries were optimized to a minimum, followed by analytical frequency calculations to confirm that no imaginary frequencies were present. NBO[71] calculations were then performed on the optimized geometries of **8** and **9**. Deletion energies (E_{del}) represent the change in energy upon zeroing the matrix elements corresponding to the lp(Pt)→p(P) donor−acceptor interactions.[72] XYZ coordinates of the optimized geometries of **8** and **9** are provided in the Supporting Information.

■ ASSOCIATED CONTENT

Ⓢ Supporting Information

Additional computational and spectral data, and crystallographic details and data in .cif format for **5**, **6**, **8**, and **9**. This material is available free of charge via the Internet at http://pubs.acs.org.

■ AUTHOR INFORMATION

Corresponding Author

*E-mail: thomasc@brandeis.edu.

Notes

The authors declare no competing financial interest.

■ ACKNOWLEDGMENTS

This material is based upon work supported by the National Science Foundation under Grant CHE-1138987. The authors thank Brandeis University for initially funding this project. C.M.T. is also grateful for a 2011 Sloan Research Fellowship.

■ REFERENCES

(1) Arduengo, A. J.; Harlow, R. L.; Kline, M. *J. Am. Chem. Soc.* **1991**, *113*, 361−363.

(2) Bourissou, D.; Guerret, O.; Gabbaï, F. P.; Bertrand, G. *Chem. Rev.* **1999**, *100*, 39−92.

(3) *N-Heterocyclic Carbenes in Transition Metal Catalysis*; Glorius, F., Ed.; Springer-Verlag: Berlin, Germany, 2007; Vol. *21*.

(4) Crudden, C. M.; Allen, D. P. *Coord. Chem. Rev.* **2004**, *248*, 2247−2273.

(5) Peris, E.; Crabtree, R. H. *Coord. Chem. Rev.* **2004**, *248*, 2239−2246.

(6) Enders, D.; Balensiefer, T. *Acc. Chem. Res.* **2004**, *37*, 534−541.

(7) Marion, N.; Díez-González, S.; Nolan, S. P. *Angew. Chem., Int. Ed.* **2007**, *46*, 2988−3000.
(8) Cowley, A. H.; Kemp, R. A. *Chem. Rev.* **1985**, *85*, 367−382.
(9) Gudat, D. *Coord. Chem. Rev.* **1997**, *163*, 71−106.
(10) Gudat, D. *Eur. J. Inorg. Chem.* **1998**, *1998*, 1087−1094.
(11) Gudat, D.; Haghverdi, A.; Hupfer, H.; Nieger, M. *Chem.—Eur. J.* **2000**, *6*, 3414−3425.
(12) Takano, K.; Tsumura, H.; Nakazawa, H.; Kurakata, M.; Hirano, T. *Organometallics* **2000**, *19*, 3323−3331.
(13) Pan, B.; Xu, Z.; Bezpalko, M. W.; Foxman, B. M.; Thomas, C. M. *Inorg. Chem.* **2012**, *51*, 4170−4179.
(14) Rosenberg, L. *Coord. Chem. Rev.* **2012**, *256*, 606−626.
(15) Day, G. S.; Pan, B.; Kellenberger, D. L.; Foxman, B. M.; Thomas, C. M. *Chem. Commun.* **2011**, *47*, 3634−3636.
(16) Pan, B.; Bezpalko, M. W.; Foxman, B. M.; Thomas, C. M. *Organometallics* **2011**, *30*, 5560−5563.
(17) Pan, B.; Bezpalko, M. W.; Foxman, B. M.; Thomas, C. M. *Dalton Trans.* **2012**, *41*, 9083−9090.
(18) Roncaroli, F.; Videla, M.; Slep, L. D.; Olabe, J. A. *Coord. Chem. Rev.* **2007**, *251*, 1903−1930.
(19) Hutchins, L. D.; Light, R. W.; Paine, R. T. *Inorg. Chem.* **1982**, *21*, 266−272.
(20) Förster, D.; Nickolaus, J.; Nieger, M.; Benkõ, Z.; Ehlers, A. W.; Gudat, D. *Inorg. Chem.* **2013**, *52*, 7699−7708.
(21) Hamilton, C. W.; Morris, D. E.; Blair, M. W.; Jenson, N. J.; Martin, R. L.; Cross, J. L.; Sutton, A. D.; Jantunen, K. C.; Scott, B. L.; Baker, R. T.; INOR 50-When is addition of X-Y to M not oxidative? *Proceedings of the 235th ACS National Meeting*, New Orleans, LA, April 6−10, 2008.
(22) Tomashevskaya, M. M.; Tunik, S. P.; Podkorytov, I. S.; Heaton, B. T.; Iggo, J. A.; Haukka, M.; Pakkanen, T. A.; Pirilä, P. L.; Pursiainen, J. *J. Organomet. Chem.* **2007**, *692*, 2911−2923.
(23) King, R. B.; Fu, W. K.; Holt, E. M. *J. Chem. Soc., Chem. Commun.* **1984**, *0*, 1439−1440.
(24) Dyer, P. W.; Fawcett, J.; Hanton, M. J.; Mingos, D. M. P.; Williamson, A.-M. *Dalton Trans.* **2004**, 2400−2401.
(25) Wang, W.; Low, P. J.; Carty, A. J.; Sappa, E.; Gervasio, G.; Mealli, C.; Ienco, A.; Perez-Carreño, E. *Inorg. Chem.* **2000**, *39*, 998−1005.
(26) Corrigan, J. F.; Doherty, S.; Taylor, N. J.; Carty, A. J. *Organometallics* **1993**, *12*, 993−995.
(27) Corrigan, J. F.; Dinardo, M.; Doherty, S.; Hogarth, G.; Sun, Y.; Taylor, N. J.; Carty, A. J. *Organometallics* **1994**, *13*, 3572−3580.
(28) Qiwang, L.; Xiang, H.; Binfang, W.; Shutang, L. *J. Organomet. Chem.* **1991**, *405*, 257−264.
(29) Tanabe, M.; Itazaki, M.; Kitami, O.; Nishihara, Y.; Osakada, K. *Bull. Chem. Soc. Jpn.* **2005**, *78*, 1288−1290.
(30) Sommovigo, M.; Pasquali, M.; Leoni, P.; Englert, U. *Inorg. Chem.* **1994**, *33*, 2686−2688.
(31) Arif, A. M.; Heaton, D. E.; Jones, R. A.; Nunn, C. M. *Inorg. Chem.* **1987**, *26*, 4228−4231.
(32) Leoni, P.; Sommovigo, M.; Pasquali, M.; Sabatino, P.; Braga, D. *J. Organomet. Chem.* **1992**, *423*, 263−270.
(33) Englert, U.; Matern, E.; Olkowska-Oetzel, J.; Pikies, J. *Acta Crystallogr., Sect. E* **2003**, *59*, m376−m377.
(34) Mealli, C.; Ienco, A.; Galindo, A.; Carreño, E. P. *Inorg. Chem.* **1999**, *38*, 4620−4625.
(35) Pauling, L. *The Nature of the Chemical Bond*, 3rd ed.; Cornell University Press: Ithaca, NY, 1960.
(36) Albinati, A.; Leoni, P.; Marchetti, F.; Marchetti, L.; Pasquali, M.; Rizzato, S. *Eur. J. Inorg. Chem.* **2008**, *2008*, 4092−4100.
(37) Gallo, V.; Latronico, M.; Mastrorilli, P.; Nobile, C. F.; Suranna, G. P.; Ciccarella, G.; Englert, U. *Eur. J. Inorg. Chem.* **2005**, *2005*, 4607−4616.
(38) Leoni, P.; Chiaradonna, G.; Pasquali, M.; Marchetti, F. *Inorg. Chem.* **1998**, *38*, 253−259.
(39) Petz, W.; Kutschera, C.; Neumüller, B. *Organometallics* **2005**, *24*, 5038−5043.
(40) Leoni, P.; Marchetti, F.; Marchetti, L.; Passarelli, V. *Chem. Commun.* **2004**, 2346−2347.
(41) Misumi, Y.; Ishii, Y.; Hidai, M. *J. Chem. Soc., Dalton Trans.* **1995**, 3489−3496.
(42) Khasnis, D. V.; Lattman, M.; Siriwardane, U.; Zhang, H. *Organometallics* **1992**, *11*, 2074−2079.
(43) Komine, N.; Hirota, T.; Hirano, M.; Komiya, S. *Organometallics* **2008**, *27*, 2145−2148.
(44) Chen, W.; Liu, F.; Nishioka, T.; Matsumoto, K. *Eur. J. Inorg. Chem.* **2003**, *2003*, 4234−4243.
(45) Bender, R.; Braunstein, P.; Bouaoud, S.-E.; Rouag, D.; Harvey, P. D.; Golhen, S.; Ouahab, L. *Inorg. Chem.* **2002**, *41*, 1739−1746.
(46) Fukuoka, A.; Fukagawa, S.; Hirano, M.; Komiya, S. *Chem. Lett.* **1997**, *26*, 377−378.
(47) Chen, W.; Matsumoto, K. *Eur. J. Inorg. Chem.* **2002**, *2002*, 2664−2670.
(48) Breuer, M.; Strähle, J. *Z. Anorg. Allg. Chem.* **1993**, *619*, 1564−1574.
(49) Adams, R. D.; Chen, G.; Wu, W.; Yin, J. *Inorg. Chem.* **1990**, *29*, 4208−4214.
(50) Khasnis, D. V.; Lattman, M.; Siriwardane, U. *Inorg. Chem.* **1989**, *28*, 2594−2600.
(51) Macklin, P. D.; Mirkin, C. A.; Viswanathan, N.; Williams, G. D.; Geoffroy, G. L.; Rheingold, A. L. *J. Organomet. Chem.* **1987**, *334*, 117−128.
(52) Kitano, K.; Tanaka, K.; Nishioka, T.; Ichimura, A.; Kinoshita, I.; Isobe, K.; Ooi, S. *J. Chem. Soc., Dalton Trans.* **1998**, 3177−3182.
(53) Gallo, V.; Mastrorilli, P.; Nobile, C. F.; Braunstein, P.; Englert, U. *Dalton Trans.* **2006**, 2342−2349.
(54) Hegmans, A.; Zangrando, E.; Freisinger, E.; Pichierri, F.; Randaccio, L.; Mealli, C.; Gerdan, M.; Trautwein, A. X.; Lippert, B. *Chem.—Eur. J.* **1999**, *5*, 3010−3018.
(55) Bender, R.; Braunstein, P.; Metz, B.; Lemoine, P. *Organometallics* **1984**, *3*, 381−384.
(56) Bachert, I.; Bartusseck, I.; Braunstein, P.; Guillon, E.; Rosé, J.; Kickelbick, G. *J. Organomet. Chem.* **1999**, *580*, 257−264.
(57) Leoni, P.; Vichi, E.; Lencioni, S.; Pasquali, M.; Chiarentin, E.; Albinati, A. *Organometallics* **2000**, *19*, 3062−3068.
(58) Berry, D. E.; Bushnell, G. W.; Dixon, K. R.; Moroney, P. M.; Wan, C. *Inorg. Chem.* **1985**, *24*, 2625−2634.
(59) Sommovigo, M.; Pasquali, M.; Marchetti, F.; Leoni, P.; Beringhelli, T. *Inorg. Chem.* **1994**, *33*, 2651−2656.
(60) Dell'Anna, M. M.; Mastrorilli, P.; Nobile, C. F.; Calmuschi-Cula, B.; Englert, U.; Peruzzini, M. *Dalton Trans.* **2008**, 6005−6013.
(61) Brunner, H.; Dormeier, S.; Grau, I.; Zabel, M. *Eur. J. Inorg. Chem.* **2002**, *2002*, 2603−2613.
(62) Edgell, W. F.; Lyford, J. *Inorg. Chem.* **1970**, *9*, 1932−1933.
(63) *Apex 2, Version 2 User Manual, M86-E01078*; Bruker Analytical X-ray Systems: Madison, WI, 2006.
(64) Frisch, M. J.; Trucks, G. W.; Schlegel, H. B.; Scuseria, G. E.; Robb, M. A.; Cheeseman, J. R.; Scalmani, G.; Braone, V.; Mennucci, B.; Petersson, G. A.; et al. *Gaussian 09*, Revision A. 1; Gaussian, Inc.: Wallingford, CT, 2009.
(65) Becke, A. D. *J. Chem. Phys.* **1993**, *98*, 5648−5652.
(66) Lee, C.; Yang, W.; Parr, R. G. *Phys. Rev. B* **1988**, *37*, 785−789.
(67) Hay, P. J.; Wadt, W. R. *J. Chem. Phys.* **1985**, *82*, 299−310.
(68) Hay, P. J.; Wadt, W. R. *J. Chem. Phys.* **1985**, *82*, 270−283.
(69) Wadt, W. R.; Hay, P. J. *J. Chem. Phys.* **1985**, *82*, 284−298.
(70) Dunning, T. H.; Hay, P. J. In *Modern Theoretical Chemistry*; Schaefer, H. F., Ed.; Plenum: New York, 1976; Vol. 3, pp 1−28.
(71) Glendening, E. D.; Reed, A. E.; Carpenter, J. E.; Weinhold, F. *NBO*, Version 3.1.
(72) Reed, A. E.; Curtiss, L. A.; Weinhold, F. *Chem. Rev.* **1988**, *88*, 899−926.

dx.doi.org/10.1021/ic4012873 | *Inorg. Chem.* 2013, 52, 9583−9589